Available online at www.sciencedirect.com

ScienceDirect

Energy Procedia 124 (2017) 120–125

Energy Procedia

www.elsevier.com/locate/procedia

7th International Conference on Silicon Photovoltaics, SiliconPV 2017

Identifying the location of recombination from voltage-dependent quantum efficiency measurements

Byungsul Min[a]*, Christian Kruse[a], Carsten Schinke[c], Martin Wolf[a], Matthias Müller[b], Hendrik Sträter[b], Matthias Wagner[b], Karsten Bothe[a], Rolf Brendel[a,c]

[a]*Institute for Solar Energy Research Hamelin (ISFH), Am Ohrberg 1, 31860 Emmerthal, Germany*
[b]*SolarWorld Innovations GmbH, Berthelsdorfer Straße 111A, 09599 Freiberg, Germany*
[c]*Dep. Solar Energy, Inst. Solid-State Physics, Leibniz University of Hannover, Appelstr. 2, 30167 Hannover, Germany*

Abstract

This paper investigates process-induced variations of the open-circuit voltage (V_{oc}) using voltage-dependent quantum efficiency measurements. By means of device modelling we show that this method is able to explain the V_{oc} difference of two solar cells, even if they show identical electrical behaviour under short-circuit condition. This paper furthermore explains how the origin of V_{oc} variations can be classified into emitter, base and rear of the solar cell. The simulation results have been experimentally verified with industrial-type passivated emitter and rear cells (PERC) cells made from p-type Czochralski wafers. The proposed analysis method is an attractive way for monitoring V_{oc} variations of solar cells in industrial mass production since there is no need for specially prepared test structures.

Peer review by the scientific conference committee of SiliconPV 2017 under responsibility of PSE AG.

Keywords: PERC; quantum efficiency; open-circuit voltage; process monitoring

1. Introduction

The open-circuit voltage (V_{oc}) is particularly sensitive to recombination losses. Variations in the recombination rate and thus in the concentration of the electrons and holes directly affect V_{oc}. Hence, an insufficient process

* Corresponding author. Tel.: +49-5151-999-644; fax: +49-5151-999-400.
E-mail address: min@isfh.de

1876-6102
Peer review by the scientific conference committee of SiliconPV 2017 under responsibility of PSE AG.
10.1016/j.egypro.2017.09.324

stability or quality may result in significant V_{oc} variations. In order to reduce such process-induced variations of V_{oc} and of the corresponding cell efficiency, it is crucial to locate that part of the device that is responsible for the deviation from the targeted V_{oc} value. We analyze the solar cell under different operation conditions, since the respective locations exhibit different injection-dependencies of the recombination rate.

In this article, we perform voltage-dependent differential quantum efficiency measurement [1-5] to explain the process-induced variations of V_{oc}. As an application, we apply our approach to industrial-type PERC cells with p-type CZ wafers. By a combination of device modelling and experiments, we demonstrate that our method allows locating the origin of V_{oc} variations.

2. Principle of the method

The key points of our method are the following: first, the absorption depth is related to the wavelength of light. For a silicon solar cell featuring a front emitter, light of wavelength 300 nm is absorbed completely in the emitter while light of wavelength 1100 nm is absorbed almost homogeneously in the entire cell as shown in Fig. 1. Hence, the quantum efficiency at 300 nm is dominated by recombination in the emitter. This characteristic will be used to distinguish the emitter from the other parts of the solar cell. Second, by analyzing the differential external quantum efficiency (EQE) under forward voltage bias we are also able to distinguish the base from the rear, because it enables to monitor the injection-dependence of the recombination losses. However, this approach requires the saturation of the recombination losses in the base by increasing voltage as shown in next section.

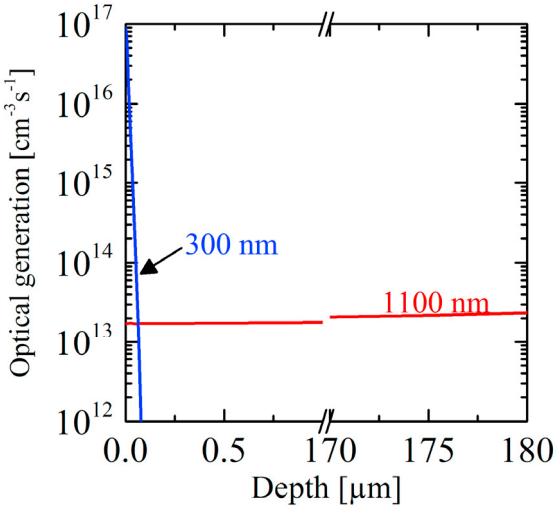

Fig. 1. Simulated optical generation for monochromatic light with wavelengths of 300 nm and 1100 nm as a function of depth from the front.

3. Modelling

We firstly simulate an industrial p-type mono-crystalline PERC cell as the reference, since the PERC design is especially sensitive to process-induced variation of device parameters such as bulk lifetime or surface passivation quality [6]. Starting from this reference cell, we model three different test cells by modifying a specific part (emitter, rear contacts and base) while the other parts of the simulated device remain identical. Compared to the reference cell, the V_{oc} values of these cells are lower (ΔV_{oc} = 5.4 ~ 7.8 mV) but their J_{sc} values are close to J_{sc} of the reference (ΔJ_{sc} < 0.2 mA/cm²). We thus consider three different origins for the V_{oc} reduction: 1) the emitter, 2) the rear contacts and 3) the base. We then simulate EQE curves of these three PERC cells with a forward bias voltage ranging from 0 to 700 mV. We model monochromatic illumination with wavelengths of 300 and 1100 nm. The intensity of the light source is equal to 1μWcm^{-2}. There is no bias light, since we do not aim to determine the

absolute EQE. For our simulation study, we use state-of-the-art SENTAURUS device modelling [7] by applying most recent device models and silicon parameters [8-10].

4. Simulation results

The simulated EQE curves strongly depend on the forward bias voltage as shown in Fig. 2. For bias voltage below 550 mV the EQE at 300 and 1100 nm are constant. They show common decrease at voltages above 550 mV. This is due to the decrease of the differential resistance of the solar cell at increasing bias voltage. As a consequence more photo-generated current is diverted through the solar cell [11]. By comparing the EQE of the three test cells (dashed lines) with the EQE of the reference cell (solid lines), we observe for case 1 that the difference between EQE is slightly greater for the light of wavelength 300 nm (blue lines) than the light of wavelength 1100 nm (red lines). In contrast, in case 2 and 3, the difference between EQE is greater for the light of wavelength 1100 nm than the light of wavelength 300 nm. Additionally, we observe in case 3 that the EQE of the test cell becomes nearly identical with the EQE of the reference cell at voltages greater than 680 mV.

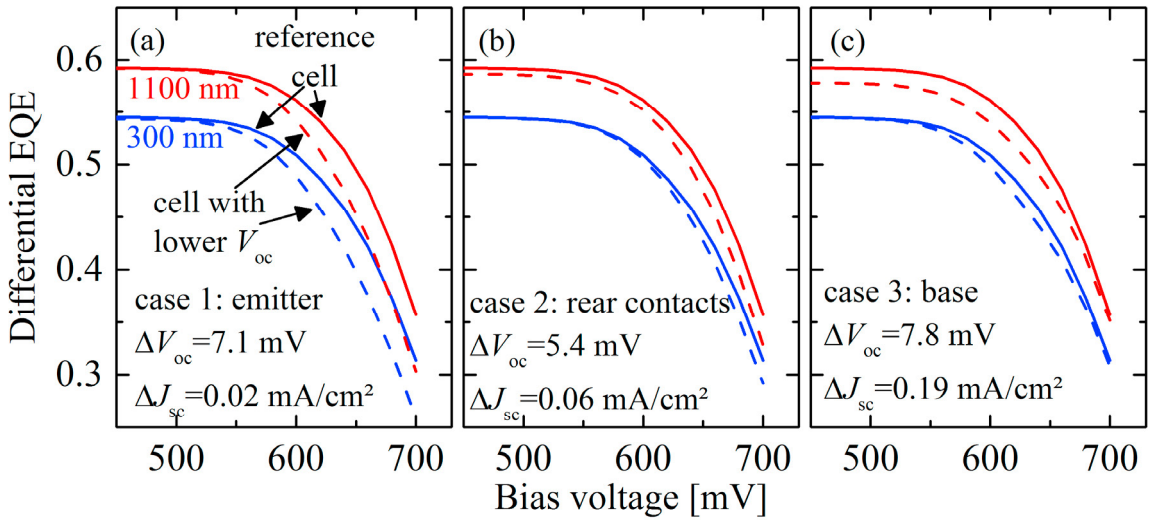

Fig. 2. Simulated EQE of the reference cell and the cells with lower V_{oc} due to increased recombination losses (a) in the emitter, (b) at rear contacts and (c) in the base.

As can be seen from Fig. 2 the change in EQE between the reference cell and the test cell is different for the three cases. Thus, in order to point out the decisive differences, we calculate the ratio between the EQE of the reference and the EQE of the test cells as shown in Fig. 3. The ratio is defined as follows:

$$Ratio(\lambda) = \frac{EQE(reference\ cell)}{EQE\ (cell\ with\ lower\ V_{OC})}\Big|_{\lambda} \quad (1)$$

Based on the comparison of the results from the different case studies we derive following criterions to determine the device part which is responsible for the V_{oc} deviation: (i) for ratio(300 nm) > ratio(1100 nm), the deviation of V_{oc} is caused by increased recombination losses in the emitter (case 1), since the EQE at 300 nm responds more sensitively to the recombination in the emitter; (ii) for ratio(300 nm) < ratio(1100 nm), the V_{oc} deviation is caused by increased recombination losses in the base or at rear (case 2 and 3), because the EQE at 1100 nm is dominated by recombination in the base and at rear; (iii) if the ratio of both wavelengths decrease towards 1 at voltages near 700 mV, the deviation of V_{oc} is caused by increased recombination losses in the base. This effect can be explained by the recombination saturation in the base region due to asymmetric capture cross-sections of defects such as iron-boron [12] or boron-oxygen complex [13] as shown in Fig. 4.

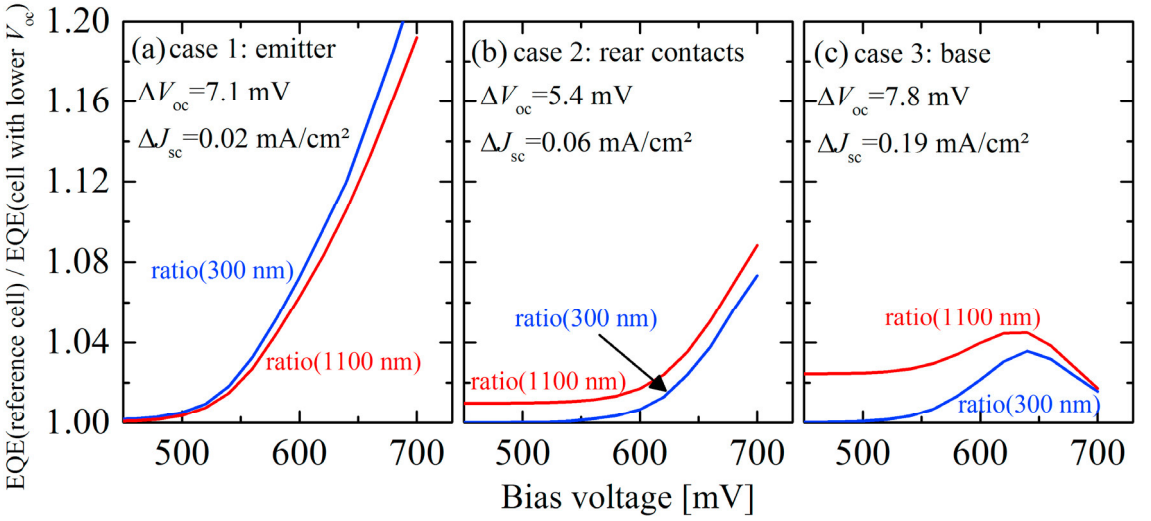

Fig. 3. Ratio between the simulated EQE of the reference cell and the simulated EQE of the cells with lower V_{oc} due to increased recombination losses (a) in the emitter, (b) at rear contacts and (c) in the base.

It is to note that the ratio curve will be a mixture of these three cases if multiple device parts are responsible for the V_{oc} variation. In such case, it is still possible to locate the corresponding device parts. However, it may be difficult to identify which device part is mainly responsible for the V_{oc} variation.

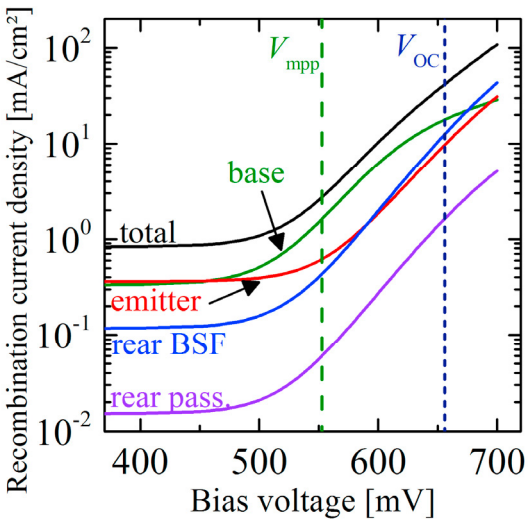

Fig. 4. Simulated recombination current densities for the reference PERC cell as a function of the operating voltage under 1-sun illumination of the various device regions. We integrate the recombination losses over emitter, base and rear region of the cell separately, multiply them by the elementary charge to obtain units of mA/cm^2.

5. Experimental validation

We apply our new method to industrial PERC cells in order to reproduce case 1 (emitter) and case 3 (base) in the previous simulation study. Therefore, we carefully choose two pairs of PERC cells where the deviation of V_{oc} is due to increased recombination losses in the emitter (pair 1) or in the base (pair 2). For the pair 1 this is ensured since its

EQE under short-circuit condition shows differences only for short wavelength region. For the pair 2 we ascertain that the V_{oc} deviation is due to different amount of interstitial iron content in the substrate by performing photoluminescence analysis.

Using an extended LOANA system from pv-tools, we measure the voltage-dependent differential quantum efficiency without bias light at 25 °C with lock-in technique. The chopper frequency is set to 375 Hz. The monochromatic light is applied to an area of slightly less than 2×2 cm². Thus, we cut 2×2 cm² samples from our solar cell in order to avoid the interaction between illuminated and non-illuminated part of the solar cell. Subsequently, we calculate the ratio between the measured EQE of the cells with different V_{oc} values as shown in Fig. 5.

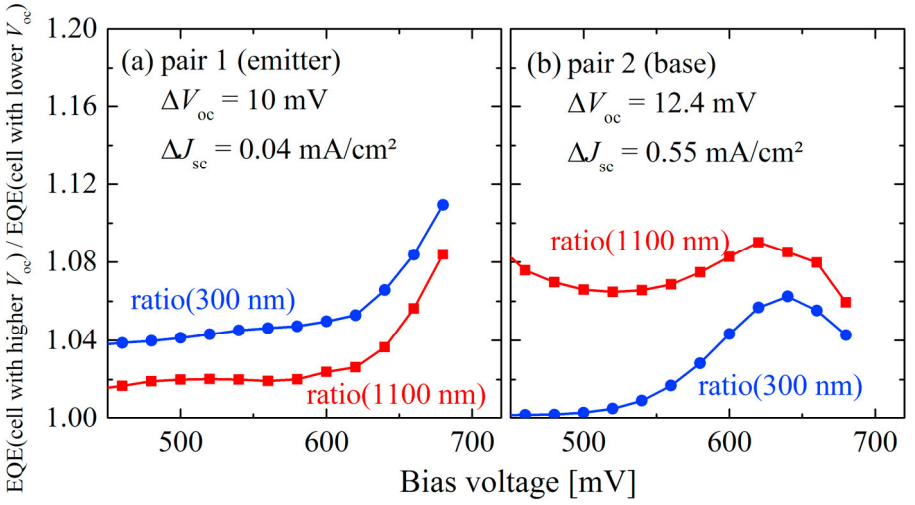

Fig. 5. Ratio between the measured EQE of the cells with different V_{oc} values due to different recombination losses in (a) the emitter and (b) the base.

By comparing Fig. 5(a) and 5(b) with Fig. 3(a) and 3(c) respectively, we successfully validate our new method, by demonstrating qualitative agreement between the shapes of the simulated and experimental curves. The curves in Fig. 5(a) correspond to Fig. 3(a) which emitter case whereas Fig 5(b) is similar to Fig. 3(c) that is the base case where the drop of the ratio towards 700mV is visible.

6. Conclusion

We develop a non-invasive characterization method for monitoring process-induced V_{oc} variations in mass production of solar cells. In order to locate the origin of V_{oc} variations we use two wavelengths of the monochromatic light source (300 nm & 1100 nm), where the absorption depth falls below the emitter depth or exceeds the substrate thickness. In contrast to the common quantum efficiency analysis under short-circuit condition we apply bias voltage up to 700 mV in order to monitor the injection-dependent recombination losses. The comparison of the voltage-dependent quantum efficiency data allows classifying the origin of V_{oc} variations into following three parts of the solar cell: emitter, base and rear.

Acknowledgements

The authors thank M. Vogt for a critical reading of the manuscript. This work was funded by the Federal Ministry for Economic Affairs and Energy (FKZ 0325777).

References

[1] R. Potter, C. Eberspacher, L. Fabick. "Device analysis of CuInSe2/(Cd, Zn) S/ZnO solar cells", Proc. of the IN: Photovoltaic Specialists Conference, 18th, Las Vegas, NV, October 21-25, 1985, Conference Record (A87-19826 07-44). New York, Institute of Electrical and Electronics Engineers, Inc., 1985, p. 1659-1664., 1985, pp. 1659-1664.
[2] S. Albright, V. Singh, J. Jordan. "Junction characteristics of CdS/CdTe solar cells", Sol. Cells 24, 43-56 (1988).
[3] J. Sites, H. Tavakolian, R. Sasala. "Analysis of apparent quantum efficiency", Sol. Cells 29, 39-48 (1990).
[4] H. Mäckel, A. Cuevas. "The spectral response of the open-circuit voltage: a new characterization tool for solar cells", Sol. Energ. Mat. Sol. 81, 225-237 (2004).
[5] L. Kreinin, N. Bordin, N. Eisenberg. "Spectral response of Si solar cells at different light and voltage bias", Proc. of the 22nd European Photovoltaic Solar Energy Conference,, Milan, Italy, 2007, pp. 1301.
[6] M. Müller, P.P. Altermatt, H. Wagner, G. Fischer. "Sensitivity Analysis of Industrial Multicrystalline PERC Silicon Solar Cells by Means of 3-D Device Simulation and Metamodeling", IEEE J. Photovolt. 4, 107-113 (2014).
[7] Sentaurus, user manual, Synopsys Inc. Mountain View, 2016.
[8] P.P. Altermatt. "Models for numerical device simulations of crystalline silicon solar cells—a review", J. Comput. Electron. 10, 314-330 (2011).
[9] A. Richter, S.W. Glunz, F. Werner, J. Schmidt, A. Cuevas. "Improved quantitative description of Auger recombination in crystalline silicon", Phy. Rev. B 86, 165202 (2012).
[10] H. Steinkemper, M. Rauer, P. Altermatt, F.D. Heinz, C. Schmiga, M. Hermle. "Adapted parameterization of incomplete ionization in aluminum-doped silicon and impact on numerical device simulation", J. Appl. Phys. 117, 074504 (2015).
[11] R. Brendel, "Thin-film crystalline silicon solar cells: physics and technology", (John Wiley & Sons, 2011).
[12] D. Macdonald, L. Geerligs. "Recombination activity of interstitial iron and other transition metal point defects in p-and n-type crystalline silicon", App. Phys. Lett. 85, 4061-4063 (2004).
[13] K. Bothe, R. Sinton, J. Schmidt. "Fundamental boron-oxygen-related carrier lifetime limit in mono- and multicrystalline silicon", Prog. Photovoltaics 13, 287-296 (2005).